Experimental characterization of coherent, radially-sheared zonal flows in the DIII-D tokamak[a)]

G. R. McKee,[b)] R. J. Fonck, and M. Jakubowski
University of Wisconsin—Madison, Madison, Wisconsin 53706

K. H. Burrell
General Atomics, P.O. Box 85608, San Diego, California 92186

K. Hallatschek
Max-Planck Institut für Plasmasphysik, Garching, Germany

R. A. Moyer and D. L. Rudakov
University of California, San Diego, La Jolla, California 92093

W. Nevins, G. D. Porter, P. Schoch, and X. Xu
Lawrence Livermore National Laboratory, Livermore, California 94551

(Received 11 November 2002; accepted 16 January 2003)

The application of time-delay-estimation techniques to two-dimensional measurements of density fluctuations, obtained with beam emission spectroscopy in DIII-D [J. L. Luxon, Nucl. Fusion **42**, 614 (2002)] plasmas, has provided temporally and spatially resolved measurements of the turbulence flow-field. Features that are characteristic of self-generated zonal flows are observed in the radial region $0.85 \leqslant r/a \leqslant 1.0$. These features include a coherent oscillation (approximately 15 kHz) in the poloidal flow of density fluctuations that has a long poloidal wavelength, possibly $m=0$, narrow radial extent ($k_r \rho_I < 0.2$), and whose frequency varies monotonically with the local temperature. The approximate effective shearing rate, dv_θ/dr, of the flow is of the same order of magnitude as the measured nonlinear decorrelation rate of the turbulence, and the density fluctuation amplitude is modulated at the frequency of the observed flow oscillation. Some phase coherence is observed between the higher wavenumber density fluctuations and low frequency poloidal flow fluctuations, suggesting a Reynolds stress contribution. These characteristics are consistent with predicted features of zonal flows, specifically identified as geodesic acoustic modes, observed in 3-D Braginskii simulations of core/edge turbulence. © *2003 American Institute of Physics.*
[DOI: 10.1063/1.1559974]

I. INTRODUCTION

Turbulent transport, which results from correlated fluctuations in plasma parameters (density, temperature, potential and magnetic field), limits energy and particle confinement in magnetic confinement devices and remains a central scientific challenge to optimizing fusion-energy systems.[1] Understanding the mechanisms that drive and saturate plasma turbulence is crucial to evaluating and optimizing experimental results and predicting performance in next-generation fusion experiments. Recent theoretical work has suggested that the saturated state of turbulence is mediated by self-generated zonal flows.[2,3]

Turbulence theory and simulations[4] predict the existence of self-generated axisymmetric ($n=0$) zonal flows that act to regulate the turbulence amplitude through the time-varying $E_r \times B_T$ flows.[5] These zonal flows exhibit a low-frequency branch, often referred to as the ''residual'' or Hinton–Rosenbluth mode,[3,6] and a related higher frequency branch, identified as geodesic acoustic modes (GAM).[7,8] These zonal flows are predicted to be toroidally and azimuthally symmetric electrostatic potential structures ($m=n=0$) with a narrow radial extent ($k_r \rho_I < 1$).

Several experimental observations that suggest the existence of zonal flows have been obtained from the measurements of edge density and potential fluctuations. Phase-contrast imaging measurements have observed a turbulent structure in the density field with a finite radial wavelength, and $k_\theta \approx 0$, as predicted by theory, hinting at the existence of zonal flows.[9] The Reynolds stress formulation of zonal flow theory can be related to a three-wave coupling problem.[10] A spatial variation of Reynolds stress may be rewritten as the turbulent velocity bispectrum $\langle \tilde{v}_\theta^*(k_z) \tilde{v}_r(k_1) \tilde{v}_\theta(k_2) \rangle$, ensemble averaged between the turbulent scales k_1 and k_2 and the zonal flow scale k_z. Measurable increases in the phase coherence between the large-scale flow field and turbulence immediately prior to an LH transition were obtained using ion saturation current and floating potential fluctuations.[10–12] The Reynolds stress has also been inferred as a generation mechanism of increased poloidal flow leading up to an L–H transition by measuring v_θ with Mach probes.[13] Radially localized, low frequency poloidally symmetric potential structures, with characteristics expected for zonal flows, have also

[a)]Paper UI2 5, Bull. Am. Phys. Soc. **47**, 325 (2002).
[b)]Invited speaker. Present address: General Atomics, P.O. Box 85608, San Diego, California 92186-5608; electronic mail: mckee@fusion.gat.com

been observed in a heliac toroidal plasma at lower temperatures where interior probe measurements are feasible.[14]

Zonal flows are time-varying $E_r \times B_T$ flows, and thus should be manifest in the poloidal flow velocity of density fluctuations, which is determined by the equilibrium and time-varying $E_r \times B_T$ flows as well as any diamagnetic flows within the plasma frame. This suggests an examination of the turbulence flow field as a more direct measure of zonal flow characteristics. Recently deployed density fluctuation imaging capability using the beam emission spectroscopy diagnostic on DIII-D[15–17] allows for the direct measurement of the time-dependent turbulence flow-field under plasma conditions with a sufficient level of ambient turbulence (approximately $\tilde{n}/n > 5\%$). The derived turbulence flow-field measurements exhibit features that are very similar to the predicted zonal flow characteristics,[18] and compare well specifically to predictions for geodesic acoustic modes seen in simulations of edge turbulence.[7] These characteristics include the mode frequency and temperature scaling of the frequency, radial and poloidal structure and some hint of the nonlinear generation mechanism. The observed flows are shown to modulate the ambient turbulence amplitude. We discuss the measurement techniques to obtain the high frequency flow measurements, the experimental conditions, measured turbulence flow field characteristics, and simulations of the discharges under investigation.

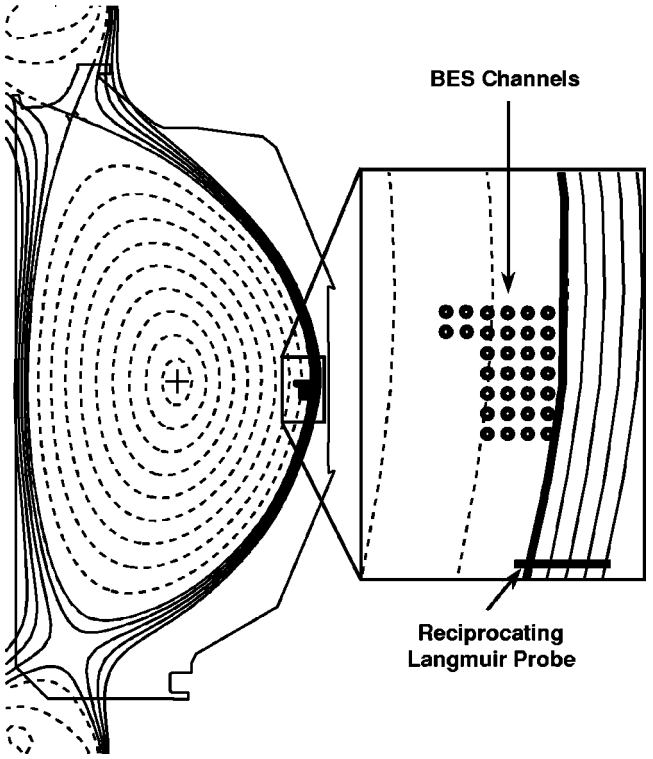

FIG. 1. Spatial locations of BES channels on the magnetic equilibrium and expanded view of the 32 channels deployed to obtain 2-D fluctuation and turbulence flow measurements near the outer midplane, and position of the reciprocating Langmuir probe.

II. FLOW-FIELD MEASUREMENT METHODS

The poloidal velocity flow-field of the convecting turbulent eddies is derived from the experimentally measured density fluctuation data using time-delay-estimation (TDE) techniques.[17–21] 2-D density fluctuation data are obtained with the DIII-D beam emission spectroscopy (BES) system.[22] BES observes density fluctuations by measuring the fluorescence from heating neutral beam atoms as they undergo excitation via collisions with plasma ions and electrons.[23] The intensity of the Doppler-shifted D_α emission ($n=3$–2 near $\lambda = 652$–655 nm) is sampled at 1 MHz[24] and yields a relative measure of the local plasma density. Each channel has a spatial resolution of about 1 cm in the radial and poloidal direction, achieved via alignment of the optical sightline and magnetic field lines at the beam–volume intersection. 32 spatially-localized viewing channels are available and have been deployed to obtain 2-D measurements over a roughly 5 cm (radial)$\times$7 cm (poloidal) spatial region at the outboard tokamak midplane ($4\times7+2\times2$ channel grid). Figure 1 illustrates the arrangement of spatial channels relative to the magnetic equilibrium for this experiment. The array was scanned radially on a shot-to-shot basis to obtain detailed profile information.

The relevant turbulence flows, which are the group velocity of the turbulent eddies and should be distinguished from bulk mass flow, are dominantly in the poloidal direction. The measured flows range in frequency from essentially steady-state up to the decorrelation rates for long wavelength density turbulence ($f > 100$ kHz). Equilibrium measurements of flow are obtained using a time-delay correlation analysis between poloidally adjacent channels with the known spatial separation.[25] The measurement of high-frequency turbulence flows has required the development of specialized time-delay-estimation (TDE) techniques and the application of these techniques to these localized density fluctuation measurements. One method utilizes wavelet-based time-delay correlations to provide measurements at a frequency up to almost the upper-frequency limit of the density spectrum itself.[19] A second technique utilizes time-resolved cross-correlation analysis, and can obtain time resolutions of about 20 μs.[17,20] For the data presented in this paper, the second technique has been utilized, though both techniques yield similar results and exhibit the turbulence flows to be discussed. Generally, the wavelet technique yields a higher frequency response, while the time-resolved cross-correlation yields higher signal-to-noise for lower-frequency flow phenomena ($f < \sim 25$ kHz). The relevant time scales for physical parameters and analysis techniques are ordered as

$$\tau_{\text{min, fluctuations}} \leqslant \tau_{\text{wavelet}} < \tau_{\text{cross-corr}} < \tau_{\text{flows}}$$

with $\tau_{\text{min,fluctuations}}$ the minimum period of the measured fluctuations, τ_{wavelet} and $\tau_{\text{cross-corr}}$ the time-resolution of the two respective analysis techniques, and τ_{flows} the period of the flow patterns to be studied.

Figure 2 illustrates the turbulence flow analysis procedure. A sample 300 μs window of 1 MHz density fluctuation data for two poloidally adjacent channels ($\Delta Z = 1$ cm, $\Delta R = 0$) is shown in Fig. 2(a). The two data sets exhibit high coherence and a finite time delay ($\tau_d \approx 3$ μs) owing to the equilibrium turbulence flow, approximately 3 km/s in this

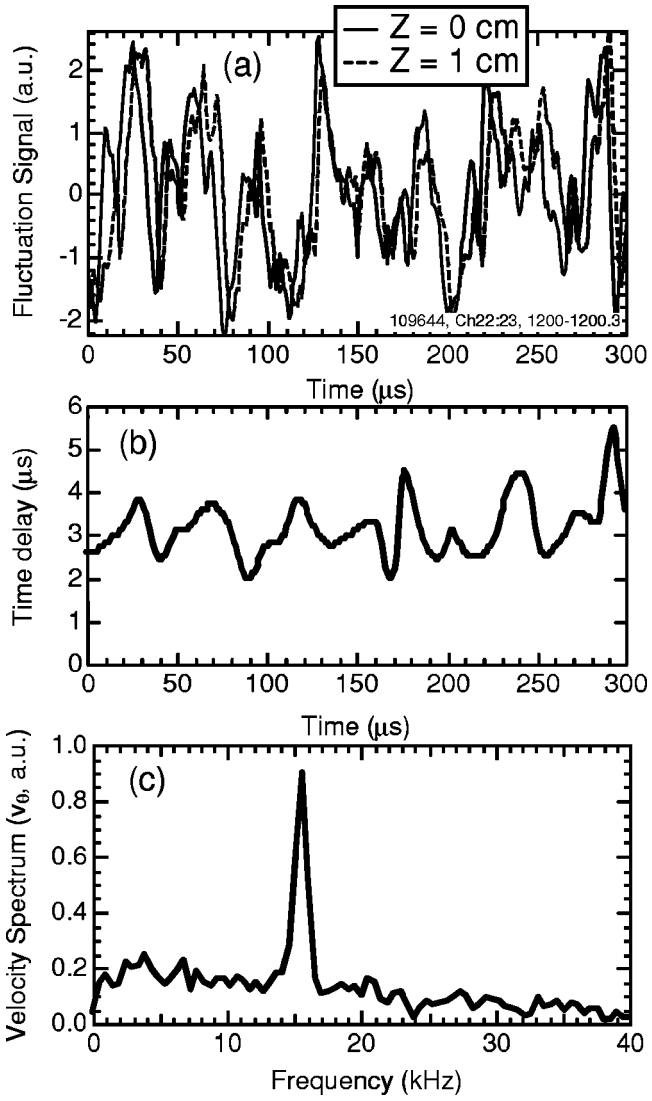

FIG. 2. (a) Sample density fluctuation measurements from two poloidally adjacent channels ($\Delta Z = 1$ cm, $\Delta R = 0$ cm) near $r/a = 0.95$; (b) the measured time-delay between two channels shown in (a); and (c) the power spectrum of the derived poloidal velocity exhibiting coherent flow oscillation near 15.5 kHz.

case. The time-dependent time-delay is measured using a time-resolved time-lag cross-correlation between the two data sets. The time-delay at peak correlation within a 20 μs window is determined, and the window is then convolved through the data to generate a time-series of time-delay data, an example of which is shown in Fig. 2(b). The velocity is simply derived as $v_\theta(t) = \Delta Z/\tau_d(t)$. An example of the ensemble-averaged power spectrum of the resulting velocity measurement is shown in Fig. 2(c). The peak near 15 kHz is evidence of a coherent poloidal oscillation, discussed in detail in the next section. The 2-D channel configuration shown in Fig. 1 then allows for a measure of $v_\theta(t)$ over a 4 cm (radial)$\times$6 cm (poloidal) grid, providing a measure of $v_\theta(r,Z,t)$ that is analyzed to determine the spatial structure of the observed flow patterns.

III. CHARACTERISTIC OF MEASURED TURBULENCE FLOWS

A series of L-mode discharges on DIII-D were studied to investigate the existence of zonal flow features, as well as to measure their spatio-temporal characteristics and scaling properties. The plasmas were upper-single null discharges with nominal parameters of $I_p = 1.2$ MA, $B_T = -2.0$ T, $n_{e0} \approx 3.3\times 10^{19}\text{m}^{-3}$, $T_{e0} \approx 2.7$ keV, $T_{i0} \approx 3.5$ keV. The injected neutral beam power was varied from 2.5–7.5 MW to adjust plasma temperature. The density and flow fluctuation measurements discussed below were obtained from $t = 800$–1300 ms in the radial range $0.85 \leqslant r/a \leqslant 1.0$. Here, the ambient turbulence amplitude is relatively large ($\tilde{n}/n \geqslant 5\%$), allowing for application of the TDE analysis techniques with reasonable signal-to-noise. The edge collisionality is of order unity, though it varies strongly with radius. A series of similar discharges were run to vary the plasma temperature and density to investigate scaling properties of the measured flow characteristics.

A. Observation of a coherent poloidal flow oscillation

Spectral analysis of the $v_\theta(t)$ measurements was shown in Fig. 2(c). The v_θ spectrum exhibits a coherent oscillation near 15 kHz superimposed on a broadband feature. The mode amplitude is approximately 10% of the equilibrium poloidal flow velocity of turbulence, which itself is typically comparable to the $E_r \times B_T$ velocity. The coherent 15 kHz oscillation is not associated with any MHD activity, which was negligible in the early phase of these modest power L-mode discharges.

B. Spatial phase relationship of coherent flow mode

Figure 3(a) shows the measured phase relationship of the approximately 15 kHz v_θ oscillation across the observed spatial region. Poloidally, the v_θ structure shows little or no measurable phase shift, suggesting a long-poloidal wavelength, low-m structure ($k_\theta \approx 0$). The limited poloidal extent of the measurements and their respective uncertainty indicates that $|m| < 2$ if a uniform poloidal perturbation is assumed. Radially, the flow structure exhibits a rapid phase shift, undergoing a full 180 deg change over about 3 cm. Figure 3(b) shows the inferred 2-D flow field of the 15 kHz v_θ oscillation at one point in time. This is obtained by calculating the ensemble-averaged time-delay cross-correlation of v_θ near the mode frequency between a reference (central) channel and all others across the 2-D array. A 1 ms movie has similarly been obtained from a 100 ms time window of v_θ measurements, which helps to visualize the radial shear and poloidal uniformity of this coherent flow oscillation.

This radially-sheared flow can in principle shear the turbulent eddies, given sufficient amplitude and sufficiently low frequency.[5] Estimates of the shearing rate have been derived from the measured amplitude and spatial structure. They are comparable to, though somewhat less than, the decorrelation rate of the turbulence, qualitatively indicating that the flow shear is of sufficient amplitude to mediate the turbulence amplitude.[18]

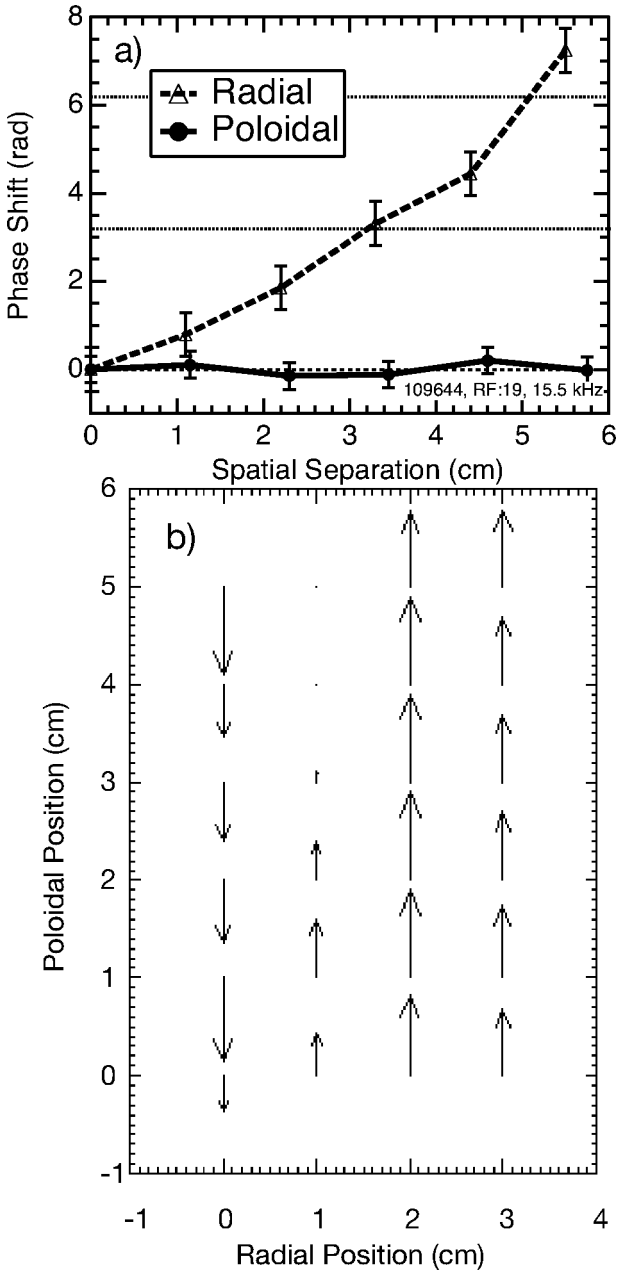

FIG. 3. (a) Radial and poloidal phase relationship of coherent v_θ oscillation at 15.5 kHz relative to the measurement at the upper, inside corner of a 2-D array; little poloidal but significant radial phase shift observed; (b) sample snapshot of a 2-D flow field of 15.5 kHz v_θ oscillation, inferred from ensemble-averaged 2-D cross-correlation.

C. Temperature dependence of flow mode frequency

The coherent v_θ oscillation, the poloidally uniform structure, and radially oscillating nature show remarkable consistency with features predicted for geodesic acoustic modes (GAMs), a class of higher-frequency zonal flow observed in simulations of edge turbulence.[7] These simulations of turbulence in the edge to core transitional regime[7] predict that the frequency of GAMs depends on temperature. Specifically, GAM frequencies are predicted to scale with the sound speed as $f_{\mathrm{GAM}} \approx c_s/2\pi R_{\mathrm{major}}$, with $C_s = \sqrt{(T_e+T_i)/M_1}$. Calculating this frequency for these discharges yields $f_{\mathrm{GAM}}=13$ kHz, very close to the observed

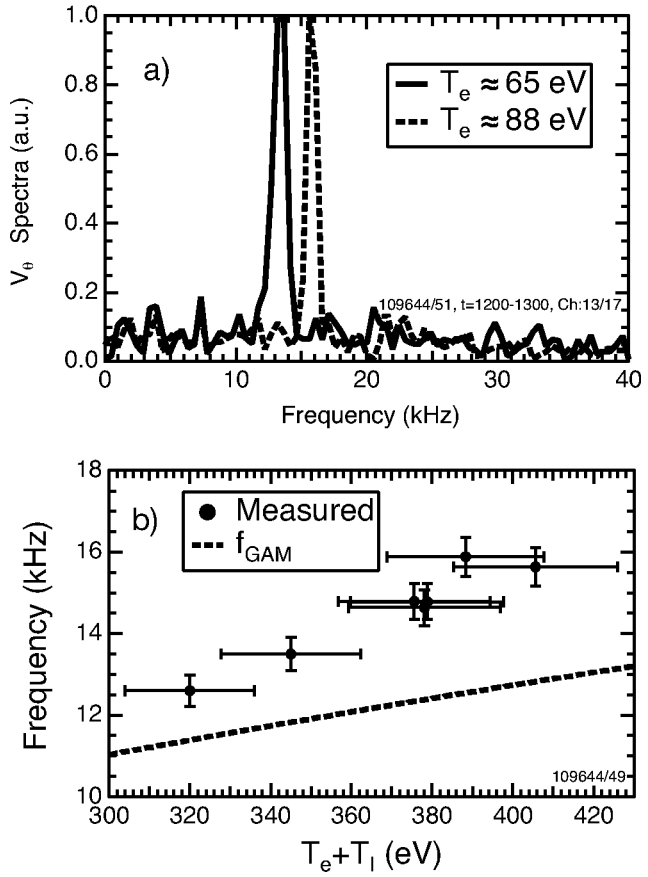

FIG. 4. (a) Two v_θ power spectra near $r/a=0.95$ in plasmas with different temperatures, and (b) the coherent mode frequency vs local temperature (T_e+T_i), and a comparison to calculated GAM frequency.

frequency. To test this prediction further, and examine whether the observed poloidal flow oscillations are GAMs, the temperature scaling of the v_θ oscillation frequency was determined. Figure 4(a) shows the poloidal velocity spectra from two discharges, measured at the same spatial location and discharge time, but with different local temperatures, demonstrating a monotonic dependence of mode frequency on temperature. Figure 4(b) shows the mode frequency versus electron plus ion temperature at several plasma conditions, along with the calculated GAM frequency. The magnitude and monotonic dependence of frequency on temperature is a further indication that the observed oscillation is a geodesic acoustic mode. Note that the GAM frequency above is approximate; the frequency observed in simulations is corrected by terms of order unity arising from plasma shape, T_e/T_i ratio, aspect ratio and poloidal rotation.[7]

D. Modulation of fluctuation amplitude by coherent flow

Zonal flows generally are predicted to regulate the amplitude of turbulence (and resulting transport) in the fully saturated state. The poloidal flow shear[26–28] from the GAMs observed here is in principle of sufficient amplitude to affect the turbulence. The effective shearing rate[29,30] of the turbulence is estimated as $\omega_s \approx dv_\theta/dr$ with v_θ referring to the poloidal velocity of the turbulent eddies that results from the

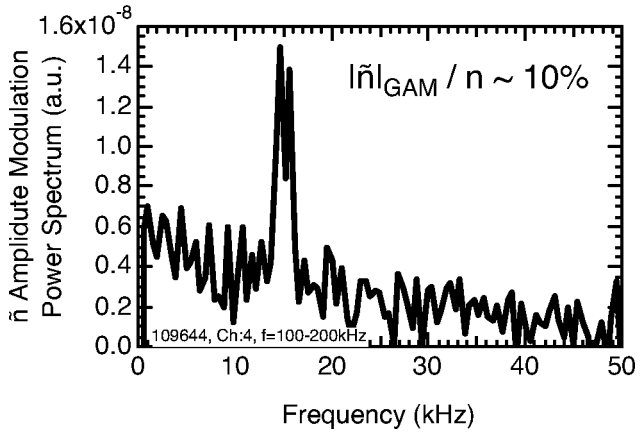

FIG. 5. Power spectrum of the amplitude modulation envelope of higher frequency density fluctuations ($100<f<200$ kHz), showing turbulence modulation at GAM oscillation frequency.

GAM oscillation. The GAM velocity amplitude is measured to be approximately 10% of the equilibrium poloidal flow velocity, which is itself about 3–5 km/s for these discharges. The radial wavenumber of the flow oscillation is about 1 cm^{-1}, so the shearing rate can be estimated as $\omega_s \approx dv_\theta/dr \approx 2(500\ \mathrm{m/s})/3\ \mathrm{cm} = 0.3\times 10^5 \mathrm{s}^{-1}$. The measured nonlinear decorrelation rate of the turbulence is $1/\tau_c \approx 1\times 10^5\ \mathrm{s}^{-1}$, thus somewhat higher, but comparable to the GAM shearing rate. Since the shear and decorrelation rates are comparable, though $\omega_s < 1/\tau_c$, it is reasonable to expect that shear in the flow oscillation can affect the ambient state of the turbulence.[5] Indeed it would be odd if $\omega_s > 1/\tau_c$ since the shear would then appear to be sufficiently large to reduce or suppress the turbulence, which clearly is not the case in this spatial region of these discharges.

The amplitude of the broadband density fluctuations is modulated at the GAM frequency. Figure 5 shows the power spectrum of the modulation envelope of the higher frequency fluctuations. Here, the locally measured density fluctuations from BES are frequency-filtered to select the broadband fluctuations in the range 100 kHz$<f<$200 kHz. This frequency range is chosen to be sufficiently above the GAM frequency and within the turbulent spectrum, which extends up to about 250 kHz. For these fluctuations, the GAM can be considered a nearly steady state flow shear. The amplitude envelope is then calculated using the Hilbert transform, with Fig. 5 then showing the Fourier power spectrum of the envelope of the frequency-filtered data. A clear peak is observed near the GAM frequency of 15 kHz. A background equal to the power spectrum of the envelope of purely Gaussian (random) fluctuations in the same frequency range and with the same total fluctuation power has been subtracted to obtain the displayed spectrum. The peak near the GAM frequency (14–16 kHz) illustrates that the amplitude of higher frequency fluctuations is being modulated by the GAM poloidal flow oscillation. For lower frequency fluctuations, the modulation is less apparent. This is consistent with the notion that a time-varying poloidal flow shear will have more effect on modes of higher frequency than the oscillation itself.[5] The amplitude of the fluctuation modulation is estimated to be about 10% of the time-averaged fluctuation amplitude, demonstrating that the GAM has a measurable effect on the ambient turbulence amplitude. The data here are integrated from 800–1300 ms of the discharge, over which time the GAM frequency increases, resulting in the broadening of the modulation frequency seen in Fig. 5. This effect is consistent with a description of the interaction between zonal flows and turbulence whereby energy is exchanged between zonal flow kinetic energy and fluctuation energy in a system that conserves total energy.[31] Here, the zonal flow (GAM) kinetic energy is oscillating coherently, as is the total fluctuation energy, qualitatively suggesting that such an energy exchange is taking place.

E. Nonlinear coupling of density fluctuations to flow mode

Zonal flows, including GAMs, are predicted to be self-generated by the turbulence itself. One mechanism by which this occurs is the radial gradient in the Reynolds stress.[32,33,11,12] The Reynolds stress $\langle \tilde{v}_r \tilde{v}_\theta \rangle$ can couple energy nonlinearly from higher wavenumber fluctuations to low ($k_\theta \approx 0$) poloidal wavenumber zonal flows. One method to experimentally measure the degree of nonlinear coupling, in lieu of a direct measurement of the Reynolds stress itself,[13] is to examine the bicoherence between high frequency density fluctuations and the electrostatic potential or velocity fluctuation.[10,11] Figure 6 shows the bicoherence measured between the coherent poloidal turbulence flow and the higher frequency density fluctuations. A broad peak is observed in the 5–25 kHz range, qualitatively indicating some degree of phase coherence between the density fluctuations in this frequency range and the turbulence flow at the sum and difference frequencies. While it does not demonstrate that the observed flow is driven solely by the Reynolds stress, it does indicate that this is a plausible mechanism contributing to the generation of the observed geodesic acoustic modes.

F. Density perturbation associated with GAM flow oscillation

A small but measurable density fluctuation is also observed to be correlated with the poloidal flow oscillation itself. The total density fluctuation spectra measured near $r/a = 0.90$ and $r/a = 0.98$ with BES are shown in Figs. 7(a) and 7(b), respectively. The density fluctuation at the 15 kHz GAM frequency is quite apparent at $r/a = 0.90$, but has either disappeared or is too small to observe at $r/a = 0.98$. The observed density fluctuations at the GAM frequency at $r/a = 0.90$ have a relatively small amplitude of $\tilde{n}/n \approx 0.25\%$. Note that this feature has no direct relationship to the amplitude modulation shown in Fig. 5, which shows the modulation of higher frequency fluctuations.

The density fluctuation exhibits a finite phase shift in the poloidal direction (as well as in the radial direction), in contrast to the turbulence poloidal flow oscillation, which exhibits essentially zero poloidal phase shift. The poloidal phase relation is shown in Fig. 7(c). The GAM density fluctuation is estimated to have $m \approx 10$, assuming a uniform poloidal perturbation and extrapolating the measured phase shift (over

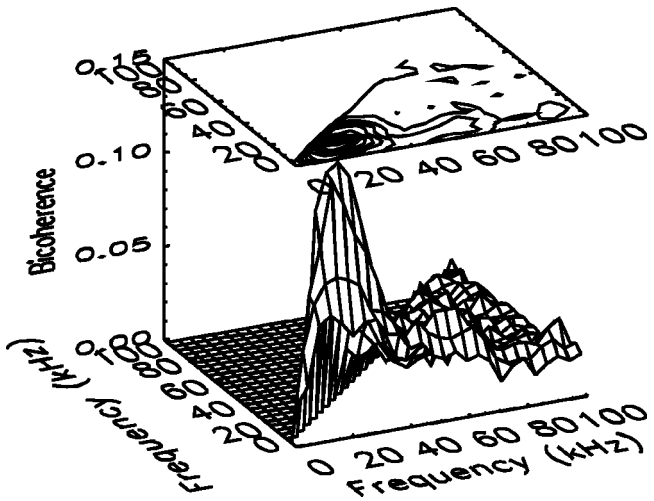

FIG. 6. Bicoherence spectrum between density fluctuations and derived velocity fluctuations, $\hat{b}^2=|\langle n_{f_1} n_{f_2} v_\theta\rangle|/(\langle n_{f_1} n_{f_2}\rangle\sqrt{\langle v_\theta v_\theta^*\rangle})$.

6 cm) around the poloidal extent of the tokamak plasma. This GAM density perturbation is observed to propagate in the electron diamagnetic direction, as seen in the lab frame, in contrast to the broadband density fluctuations, which propagate in the ion diamagnetic direction (again as seen in the lab frame). The large $E\times B$ rotation is also in the ion diamagnetic direction and dominates poloidal flow, so it cannot be determined outside the measurement uncertainty if the broadband fluctuations are convecting in the ion or electron direction in the plasma frame ($E\times B=0$). The GAM perturbation thus clearly propagates in the electron diamagnetic direction in the plasma frame.

GAMs are predicted to result from a coupling of an $m=1$, $n=0$ pressure perturbation to the toroidal magnetic geometry. The poloidal mode number, m, from the measured density fluctuation, if we assume it is indicative of the pressure perturbation, is significantly higher than this theoretically expected value. This might arise due to nonlinear coupling of the fundamental pressure oscillation to higher m modes, but should be reconciled with relevant theory.

G. Langmuir probe measurements of potential and I_{sat} fluctuations

These zonal flow features have been observed in the flow-field of the density fluctuations and are believed to be associated with the oscillating potential and corresponding $E_r\times B_T$ fluctuations of the GAM. To investigate this, potential fluctuations were measured directly with the reciprocating Langmuir probe[34] just inside the last closed flux surface. In a relatively low power discharge ($P_{inj}=2.5$ MW), the probe was inserted to approximately $r/a=0.98$, though equilibrium reconstruction uncertainties prevented a precise location determination.

The probe independently measured both the floating potential and I_{sat} ($I_{sat}\propto n_e\sqrt{T_e}$) fluctuations. The spectra for each are shown in Figs. 8(a) and 8(b). The floating potential [Fig. 8(a)] shows a coherent potential fluctuation near 12.5 kHz at $t=1500$ ms, slightly later in the discharge than when the BES flow measurements were obtained. Figure 8(b) indicates that there are little or no density (I_{sat}) fluctuations at the same frequency. This is consistent with the expectation that the GAM oscillation is a potential fluctuation with little or no associated density perturbation. Recall that the BES measurements showed no detectable density fluctuation at the GAM frequency near the separatrix [Fig. 7(b)], while a modest fluctuation was observed deeper in the plasma. The density and potential fluctuation seen at 6.5 kHz appear to not be associated with the GAM. The probe measurements thus indicate a localized floating potential fluctuation at the GAM frequency. It is thus reasonable to expect an associated radial electric field and resulting $E_r\times B_T$ oscillation of the

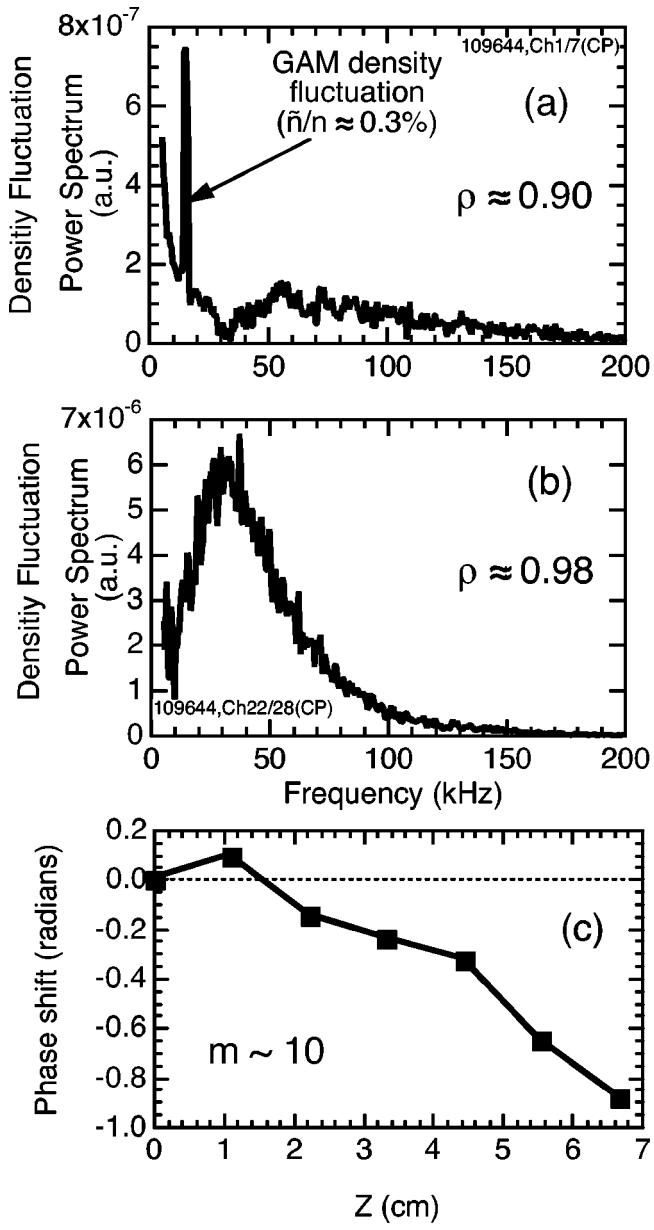

FIG. 7. (a) Density fluctuations near $r/a\approx 0.90$ associated with the GAM poloidal velocity oscillation, showing measurable density or pressure perturbation, and (b) density fluctuation spectrum near $r/a\approx 0.98$ showing no apparent fluctuation; (c) poloidal phase shift of density perturbation at $r/a\approx 0.9$ showing a finite m number ($m\sim 10$).

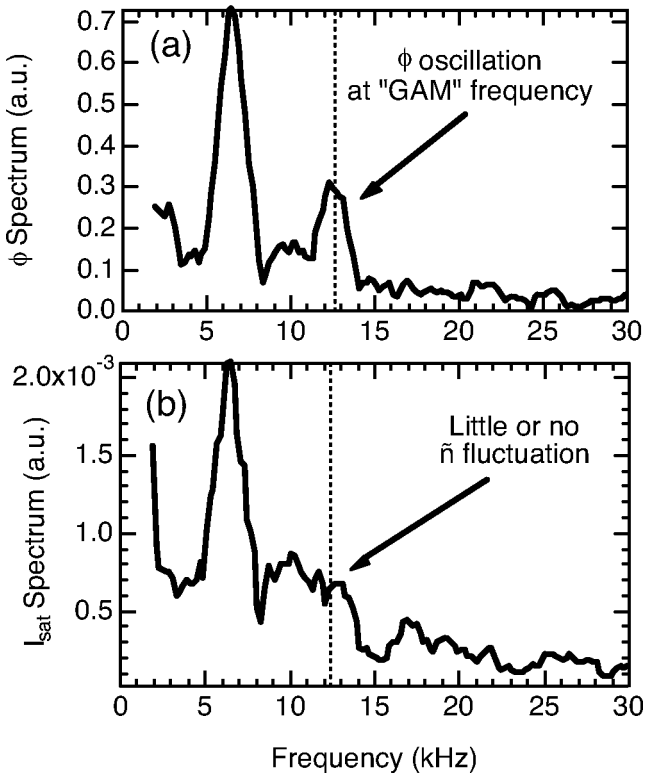

FIG. 8. (a) Measured electrostatic floating potential power spectrum, and (b) measured I_{sat} power spectrum from a reciprocating Langmuir probe inside the last closed flux surface at $t=1500$ ms; measurable potential, but little or no density (I_{sat}) fluctuation near v_θ mode frequency at 12.5 kHz.

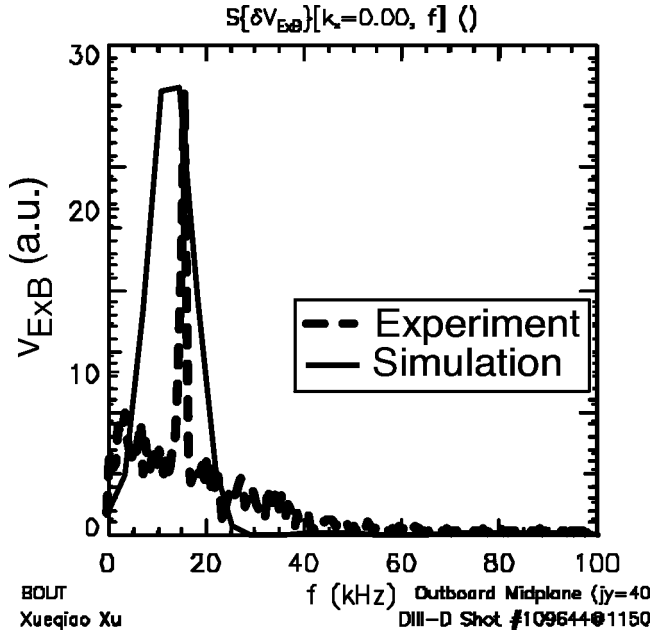

FIG. 9. A comparison of a GAM $E\times B$ oscillation observed in a BOUT simulation of experimental discharge (109644) and a comparison with measured turbulence poloidal velocity spectrum [Fig. 2(c)].

turbulence flow at this frequency, consistent with the BES flow measurements. Note that electron temperature fluctuations were also measured.[35] The plasma potential fluctuations (not shown) were calculated using the measured floating potential and T_e fluctuations and clearly show the 12.5 kHz fluctuation.

IV. SIMULATIONS AND COMPARISON WITH MEASUREMENTS

Simulations of turbulence in the outer and edge regions of the confined plasma exhibit zonal flow characteristics that are qualitatively and quantitatively similar to the turbulence flows shown here. 3-D Braginskii simulations of the edge to core transition region[7] indicate that zonal flows regulate the turbulence in this region through time-varying $E\times B$ flows. These zonal flows are specifically identified as geodesic acoustic modes (GAM), driven by a Reynolds stress and/or Stringer–Winsor mechanism, that result from $m=1$, $n=0$ pressure perturbations in the toroidal geometry. These GAMs have zonal flow features of poloidal and toroidal symmetry ($m=n=0$), radial localization, and are temporally and radially coherent. These features are very similar to the previously discussed experimental results. The experimentally measured frequencies were shown to have similar magnitude and temperature scaling to the predicted GAM frequencies (Fig. 4). The poloidal structure is shown to have little phase shift which is consistent with a very low-m, possibly $m=0$, structure. The toroidal structure cannot be determined since the measurements are available at one toroidal angle.

BOUT simulations[36] have been performed for these discharges using the experimentally measured plasma profiles and equilibrium reconstruction. A GAM oscillation is observed at nearly the same frequency as the measured value, as shown in Fig. 9. Here the potential oscillation spectrum is shown rather than the density flow oscillation that is measured with BES. The simulation was run for the equivalent of about 240 μs of discharge time (due to computational limitations) which is just over three periods of the 15 kHz oscillation, thus leading to the apparent frequency broadening of the simulation spectrum. This comparison is between the measured and simulation frequency but does not compare amplitude, which was difficult due to the short time window of the simulation. Nevertheless, the close quantitative agreement between the experimentally observed and simulated frequency of the feature suggests that the same phenomenon, which has many characteristics of a geodesic acoustic mode, is being observed.

V. SUMMARY

A coherent oscillation in the poloidal flow of density fluctuations that shows remarkable similarity to predicted characteristics of geodesic acoustic modes, a class of higher frequency zonal flows, has been observed using BES on DIII-D. The measurements were obtained by applying time-delay-estimation analysis to spatially-resolved density fluctuation measurements obtained with BES. These analysis techniques allow tracking of the turbulent eddy flow-field and resulting measurement of $v_\theta(R,Z,t)$ of the turbulence. Two methods of analyzing the data, one based on wavelets and one based on time-resolved cross-correlation, reveal similar features in the resulting flow field.

The observed poloidal flow oscillation shows a uniform poloidal structure indicating that it is a very low m, possibly $m=0$ feature. Radially, the flow changes phase by 180° over about 3 cm, a distance comparable to or somewhat larger than the turbulence radial correlation length. This flow oscillation exhibits a radial flow shear magnitude that is comparable to the decorrelation rate of the turbulence, thereby providing a mechanism to regulate the turbulence. The amplitude of the higher frequency density fluctuation ($100<f<200$ kHz) exhibits an amplitude modulation at the flow oscillation frequency of 15 kHz, indicating that the flow oscillation directly affects the turbulence amplitude. Some degree of nonlinear coupling is qualitatively shown by the finite bicoherence, or phase coupling, between the broadband density fluctuations and the flow oscillation. Langmuir probe measurements indicate that there is a potential fluctuation near the edge separatrix at the same frequency as the flow oscillation, but with little or no accompanying density (I_{sat}) oscillation. BOUT simulations performed with the measured discharge parameters show a GAM oscillation at the experimentally observed frequency.

These features also show remarkable similarity to results obtained from a recent analysis of heavy ion beam probe (HIBP) data obtained in the TEXT tokamak.[37] The HIBP results demonstrate the existence of a radially-localized $m=0$ potential fluctuation whose frequency scales with the predicted GAM frequency. Likely, a similar zonal flow phenomenon was observed in the mid-radial regions of TEXT as is being observed here near the outer regions of the DIII-D tokamak.

These experimental observations and the corresponding simulations provide compelling evidence that geodesic acoustic modes, a class of zonal flows, are active in the turbulence in the outer regions of tokamak plasmas and play an integral role in affecting and mediating the fully saturated state of turbulence and resulting transport.

ACKNOWLEDGMENTS

The authors would like to thank P. Diamond, T. S. Hahm, C. Holland, P. Terry, G. Tynan, and M. Zarnstorff for helpful discussions and suggestions. They would also like to thank the DIII-D team for support of these experiments.

This work was supported by the U.S. Department of Energy under Grants No. DE-FG02-89ER53296 and No. DE-FG03-95ER54294 and Contracts No. DE-AC03-99ER54463 and No. W-7405-ENG.

[1] B. A. Carreras, IEEE Trans. Plasma Sci. **25**, 1281 (1997).
[2] P. H. Diamond, M. N. Rosenbluth, F. L. Hinton *et al.*, *Proceedings of the 17th IAEA Fusion Energy Conference, Yokohama, 1998* (IAEA, Vienna, 2001).
[3] M. N. Rosenbluth and F. L. Hinton, Phys. Rev. Lett. **80**, 724 (1998).
[4] Z. Lin, T. S. Hahm, W. W. Lee *et al.*, Science **281**, 1835 (1998).
[5] T. S. Hahm, M. A. Beer, Z. Lin *et al.*, Phys. Plasmas **6**, 922 (1999).
[6] F. L. Hinton and M. N. Rosenbluth, Plasma Phys. Controlled Fusion **41**, A653 (1999).
[7] K. Hallatschek and D. Biskamp, Phys. Rev. Lett. **86**, 1223 (2001).
[8] T. S. Hahm, K. H. Burrell, Z. Lin *et al.*, Plasma Phys. Controlled Fusion **42**, A205 (2000).
[9] S. Coda, M. Porkolab, and K. H. Burrell, Phys. Rev. Lett. **86**, 4835 (2001).
[10] P. H. Diamond, M. N. Rosenbluth, E. Sanchez *et al.*, Phys. Rev. Lett. **84**, 4842 (2000).
[11] G. R. Tynan, R. A. Moyer, and M. J. Burin, Phys. Plasmas **8**, 2691 (2001).
[12] R. A. Moyer, G. R. Tynan, C. Holland, and M. J. Burin, Phys. Rev. Lett. **87**, 135001 (2001).
[13] Y. H. Xu, C. X. Yu, J. R. Luo *et al.*, Phys. Rev. Lett. **84**, 3867 (2000).
[14] M. G. Shats and W. M. Solomon, Phys. Rev. Lett. **88**, 045001 (2002).
[15] C. Fenzi, R. J. Fonck, M. Jakubowski, and G. R. McKee, Rev. Sci. Instrum. **72**, 988 (2001).
[16] G. R. McKee, C. Fenzi, and R. J. Fonck, IEEE Trans. Plasma Sci. **30**, 62 (2002).
[17] G. R. McKee, R. J. Fonck, C. Fenzi, and M. Jakubowski, Rev. Sci. Instrum. **74**, 2014 (2003).
[18] M. Jakubowski, R. J. Fonck, and G. R. McKee, Phys. Rev. Lett. **89**, 265003 (2002).
[19] M. Jakubowski, R. J. Fonck, C. Fenzi, and G. R. McKee, Rev. Sci. Instrum. **72**, 996 (2001).
[20] H. C. So, Electron. Lett. **34**, 722 (1998).
[21] C. Hidalgo, M. A. Pedrosa, and B. Goncalves, New J. Phys. **4**, 51.1 (2002).
[22] G. R. McKee, R. Ashley, R. Durst, R. J. Fonck *et al.*, Rev. Sci. Instrum. **70**, 913 (1999).
[23] R. J. Fonck, P. A. Dupperex, and S. F. Paul, Rev. Sci. Instrum. **61**, 3487 (1990).
[24] R. J. Fonck, R. Ashley, R. Durst *et al.*, Rev. Sci. Instrum. **63**, 4924 (1992).
[25] R. D. Durst, R. J. Fonck, G. Cosby, and H. Evensen, Rev. Sci. Instrum. **63**, 4907 (1992).
[26] K. H. Burrell, Phys. Plasmas **4**, 1499 (1997).
[27] K. H. Burrell, Science **281**, 1816 (1998).
[28] P. W. Terry, Rev. Mod. Phys. **72**, 109 (2000).
[29] T. S. Hahm and K. H. Burrell, Phys. Plasmas **2**, 1648 (1995).
[30] H. Biglari, P. H. Diamond, and P. W. Terry, Phys. Fluids B **2**, 1 (1990).
[31] P. H. Diamond, S. Champeaux, M. Malkov *et al.*, Nucl. Fusion **41**, 1067 (2001).
[32] P. H. Diamond and Y. B. Kim, Phys. Fluids B **3**, 1626 (1991).
[33] C. Holland, P. H. Diamond, S. Champeaux *et al.*, *Proceedings of the 19th IAEA Fusion Energy Conference*, Lyon, 2002 (IAEA, Vienna, 2003).
[34] J. Watkins, J. Salmonson, R. Doerner, R. Lehmer, R. Moyer *et al.*, Rev. Sci. Instrum. **63**, 4728 (1992).
[35] J. A. Boedo, D. Gray, R. W. Conn *et al.*, Rev. Sci. Instrum. **70**, 2997 (1999).
[36] X. Q. Xu, W. M. Nevins, R. H. Cohen, J. R. Myra, and P. B. Snyder, New J. Phys. **4**, 53.1 (2002).
[37] P. Schoch, ''Experimental evidence of zonal flows using HIBP data,'' Phys. Rev. Lett. (submitted); Bull. Am. Phys. Soc. **47**, 298 (2002).